Interaction of a polar molecule with an ion channel

V. Levadny,[1,2] V. M. Aguilella,[1,*] M. Aguilella-Arzo,[1] and M. Belaya[3]
[1]*Departamento de Ciencias Experimentales, Universidad Jaume I, 12080 Castellón, Spain*
[2]*The Scientific Council for Cybernetics, Russian Academy of Sciences, Vavilov str. 34, 333117 Moscow, Russia*
[3]*Institute of Plant Physiology, Russian Academy of Sciences; Botanicheskaya 35, 127276 Moscow, Russia*
(Received 7 November 2003; revised manuscript received 6 April 2004; published 29 October 2004)

The binding of a polar macromolecule to a large ion channel is studied theoretically, paying special attention to the influence of external conditions (applied voltage and ion strength of solution). The molecule behavior in bound state is considered as random thermal fluctuations within a limited fraction of its phase space. The mean duration of molecule binding (residence time τ_r) is represented as the mean first passage time to reach the boundary of that restricted domain. By invoking the adiabatic approximation we reduce the problem to one dimension with the angle between macromolecule dipole and channel axes being the key variable of the problem. The model accounts for experimental measurements of τ_r for the antibiotic Ampicillin within the bacterial porin OmpF of *Escherichia coli*. By assuming that the electrical interaction between Ampicillin dipole and OmpF ionizable groups affects the fluctuations, we find that the biased residence time-voltage dependence observed in experiments is the result of the strong transversal electric field in OmpF constriction with a tilt $\sim 30°$ aside the *cis* side.

DOI: 10.1103/PhysRevE.70.041912 PACS number(s): 87.15.Aa, 82.30.Fi, 82.37.−j

I. INTRODUCTION

A proper understanding of the nature of ion channel operation is among the main goals of membrane biophysics. Channels regulate the passage of a number of different molecules through biological membranes. Their transport characteristics are studied *in vitro* by reconstituting them in planar lipid bilayers [1]. Some channels form large-diameter pores, which are the main pathway across biological membranes for metabolites and other macromolecules such as proteins, nucleic acids, antibiotics, etc. This group of "large" channels includes bacterial porins, mitochondrial channels, gap junctions, some toxins, and others. The passage of big solutes is much slower than that of small nonorganic ions (both flows occur simultaneously) and can be time resolved under particular conditions using single-channel recording techniques. The concept is simple: the passage of a macromolecule through an electrolyte-filled channel reduces (or temporarily interrupts) the ionic current induced by a voltage bias. A partial current blockage lasting a few microseconds can be resolved and the frequency of current fluctuations measured, which enables us to study the interaction between the channel and the macromolecule and makes clear properties of the latter as well as about the nature of the interaction itself. This technique, known as the Molecular Coulter Counter [2,3], has been used to characterize individual polynucleotide molecules ([4,5] and references therein) and is the basis of a promising method for DNA sequencing, either using large channels as α-hemolysin or solid-state nanopores [6–9]. This approach was also used for studying macromolecule translocation across the Outer membrane protein F (OmpF), maltoporin (LamB), and the mitochondrial porin VDAC ([10–14] and references therein). A strong specific interaction between the macromolecule and the channel was reported for all mentioned systems, as well as a considerable influence of external conditions (*p*H, ion strength of solution, applied voltage *V*) on that interaction.

We consider here the translocation of single molecules of the antibiotic Ampicillin (AP) through the channel OmpF (outer membrane protein from *Escherichia coli*), which has been studied recently, by noise analysis of ionic currents, after reconstitution of single trimeric OmpF channels into planar lipid bilayer membranes [11]. AP blocking of channel current lasting less than 1 ms was time resolved, and the average blockage time (residence time τ_r) was found to be voltage dependent, with a bell-shaped dependence peaked at some positive voltage V_p. From their results and the relative sizes of the OmpF eyelet and the AP molecule, the authors concluded that there is a binding site for AP in the channel narrow constriction. Binding has been also reported for other solutes as well as for other porins [12–14]. More, it was concluded that just binding is the main event in solute-porin interaction [11–14].

Presently, the physicochemical nature of the AP-channel binding is not clear. However, the availability of high-resolution OmpF structure [15] combined with recent progress in the simulation of the electrostatic field inside the channel ([16–22] and references therein), which predict the strong transversal electric field in the constriction zone [16,21,24], enable us to develop a specific model for this binding. Taking into account that AP is a zwitterion with a significant dipole moment, it reasonable to think that the electric interaction has to play an important role in this phenomenon (see discussion in [11,16,23]). Studying theoretically this interaction is challenging and has a twofold interest: on the one hand, it may help to evaluate the efficiency of this drug in bacteria. On the other hand, taking into account the complicated electric interactions mentioned above, it is an interesting nontrivial physical problem.

*Corresponding author. Electronic address: aguilell@exp.uji.es

We propose here a theory which explains the effect of applied voltage on τ_r and the physical source of the shift of the curve $\tau_r(V)$ towards positive voltages. Our main idea is the following. We assume the existence of binding sites (BS's) inside OmpF constriction zone. More, we put aside the question of how AP enters the constriction zone and focus on its behavior in its bound state. Then we represent AP as an elongated solid of finite size with a significant electric dipole moment. The localization and orientation of bound AP are not fixed. The stochastic thermal effects induce random wandering of AP mass center around some specific point in constriction zone as well as random rotational oscillation of its longitudinal axis. In other words we assume that bound AP molecule undergoes random thermal motion within certain domain of its phase space. AP leaves OmpF when any point of domain boundary is reached. The escape rates across different points of boundary are different due to OmpF transversal electric field and applied voltage effect on AP behavior. Assuming the adiabatic approximation we reduce the problem to a unidimensional one with the angle between AP electric dipole and channel axis, θ, being the key variable of the problem. Formally our approach corresponds to a one-binding-site–two-barrier kinetic model discussed in the case of maltoporin translocation data [14,25].

To model the BS, we describe AP-OmpF interaction as the interaction of AP dipole with OmpF charged residues. The electric field of the channel ionizable residues is computed on the basis of the OmpF atomic structure following from crystallographic data (see Protein Data Bank file 2OMF and Ref. [15]) and the apparent *p*Ka's of residues are calculated from their corresponding values in free solution (the so-called model *p*Ka's) [24]. The interaction of AP with applied voltage is described also as the interaction of AP dipole with the applied electric field. The latter affects the relative position of AP and OmpF that is described quantitatively in our theory through the variation of the initial AP orientation and the barrier height change.

To describe AP stochastic behavior inside OmpF in bound state we use the mean first passage time (MFPT) approach [26]. The interaction of molecules with protein channels is commonly treated in the framework of the classical Eyring's rate theory, as a simple first-order binding reaction [13,14]. As is known, such an approach has been successful in reproducing the main general features of adsorption-desorption processes but it fails to explain some specific details (see also in this connection the discussion in [27]). In our particular problem this classical approach cannot provide a simple physical model which might explain the shift of the peak $\tau_r(V)$. This is why we use the MFPT approach. Its advantage in our case consists in taking into account not only the dependence of energetic barriers on the applied voltage (achieved by Eyring's approach too), but also the dependence of the adsorbed particle initial state on external conditions. The MFPT approach gives a simple physical explanation of the shift of the peak $\tau_r(V)$ to positive voltages in the framework of our theory as the result of redistribution of barrier heights and AP initial orientation upon applied voltage.

A few theoretical studies dealing with the system considered here or with very similar ones have been reported. The dependence of the number of ampicillin binding events per second with the solution *p*H and salt concentration has been analyzed by Mafé and co-workers [23]. They extended T. L. Hill's theory for intermolecular interactions in a pair of binding sites by incorporating two binding ions and two pairs of interacting sites. Recently, a one-binding-site–two-barrier kinetic model with different barrier heights was developed by Schwarz *et al.* [14] to describe the sugar (maltodextrin) translocation through maltoporin channel. This system is very similar to that studied here. Its reaction on applied voltage is alike to that for AP-OmpF. To rationalize a voltage effect on the translocation Schwarz and co-workers introduced empirically the voltage dependence of binding constant. The interaction of biopolymers with narrow pores was also analyzed by Lubensky and Nelson [28] motivated by the experiments on polynucleotide translocation across protein ion channels [29]. Their treatment bears some similarities to our approach (a unidimensional microscopic model, strong interaction between the channel and the polynucleotide, a first-passage problem) but also significant differences concerning the geometry of the translocating molecule and the key role of dipole interaction in our specific system: a channel with a strong transversal electric field at its narrow constriction and a polar molecule of the size of the constriction.

II. DESCRIPTION OF THE SYSTEM

As was mentioned in the Introduction, we analyze here the interaction of OmpF with Ampicillin, motivated mainly by the experiments performed by Nestorovich and coworkers [11]. The AP-OmpF binding and the subsequent channel current blockage was described by the residence time of the drug molecule in the pore, τ_r (typically, fractions of milliseconds), and the frequency of antibiotic entrance in OmpF, ν (the number of single-molecule binding events per second, typically around 100 sec^{-1}). Both parameters depend essentially on *p*H and the applied voltage V in a nonmonotonic way. For instance, $\nu(p\mathrm{H})$ has a sharp peak at *p*H ≈ 4.5 and $\tau_r(V)$ is peaked around $V \approx 100$ mV, positive on the side of the protein addition (*cis* side).

Ampicillin is an antibiotic with molecular weight 349.4, having a COOH^- group with *p*Ka 2.5 and a NH_4^+ group with *p*Ka 7.3 [30] separated ~ 0.9 nm (for its totally extended conformation). A crude estimation of its dipolar moment from this separation distance gives ~ 43 D and more accurate computations using GAUSSIAN'98 yield a dipolar moment of 30.8 D. In any case, AP hydration and its confinement in the pore constriction may alter these values, which should be regarded as an approximation. Thus, AP can be treated as polar zwitterion molecule with a dipole moment $\mathbf{d}_{\mathrm{AP}}$ and negligibly small net electric charge q_{AP} for *p*H $\sim 3-7$. Outside this *p*H range AP may be negatively or positively charged. The main contribution to $\mathbf{d}_{\mathrm{AP}}$ comes from carboxyl and ammonium groups; therefore, q_{AP} and $\mathbf{d}_{\mathrm{AP}}$ are determined mainly by their ionization state and by AP conformation.

OmpF is a general diffusion porin present in the outer membrane of *Escherichia coli*. As a channel, it allows the passage of ions and solutes up to a mass of about 650 Da. Its

crystal structure has been determined and has revealed that OmpF channels are trimers of identical subunits [15]. The pore exhibits an hourglass shape, with a narrow constriction (around 0.9 nm long and cross section 0.7×1.1 nm) at the center of the channel. Acidic and basic residues in the channel eyelet give rise to a strong transverse electrostatic field. Recent simulations have shown that this field could align dipolar molecules as α-methylglucose and alanine in the constriction region of OmpF [21].

Before attempting to model the AP-OmpF interaction, it is worth to take advantage of the available structural information of the channel and characterize the constriction from the electrostatic point of view: some information about the electric field at the channel constriction may give valuable clues for the subsequent modeling. Recent progress in Brownian dynamics simulations [19] proved to reproduce satisfactory the electrophysiological characteristics of big channels. Here we calculated the electric field distribution inside OmpF by taking as input the atom coordinates of the OmpF trimer obtained from its crystal structure [15], and using the UHBD code (which implements a nonlinear Poisson-Boltzmann equation solver) [31] we have calculated the electric field space distribution inside the pore. The initial grid was spaced 0.25 nm, with successive focusing down to 0.05 nm in the constriction zone. Charges were assigned from the CHARMM force field values for proteins. The ionization states of all residues correspond to the "null model"—i.e., those in free solution at *p*H 7—except for Glu296 and His21 which were corrected according to previous results for *p*Ka shifts in this system. The protein surface was first computed with MSMS [32] and graphically represented with DINO [33]. As an example, Fig. 1 shows a contour plot of the electric potential in the vicinities the channel constriction, together with a vectorial representation of the electric field. The shaded region corresponds to the protein. Computations reveal a strong transversal electric field about ~0.2 V/nm at the channel constriction where BS is presumably located (for electrolyte concentration $C_{\mathrm{KCl}}=1$ M). The field magnitude and its tilt with respect to channel axis change from ~0.15 V/nm at the ends of the constriction till 0.24 V/nm in the central part and from $\sim60°$ until $\sim110°$ along the constriction, respectively. The electric field outside this zone is an order of magnitude lower ~0.01 V/nm. Without doubt the heterogeneity of electric field distribution itself has to be on some importance for the phenomena considered here. But we believe that it is a the second-order effect and at the same time the main characteristics of this phenomenon are determined by the average value of the field. This is the reason why we used here a simplified picture of the electric field in the OmpF constriction zone, describing it by two parameters—namely, by average absolute value E_{om} and its tilt with respect to channel axis change θ_{om}.

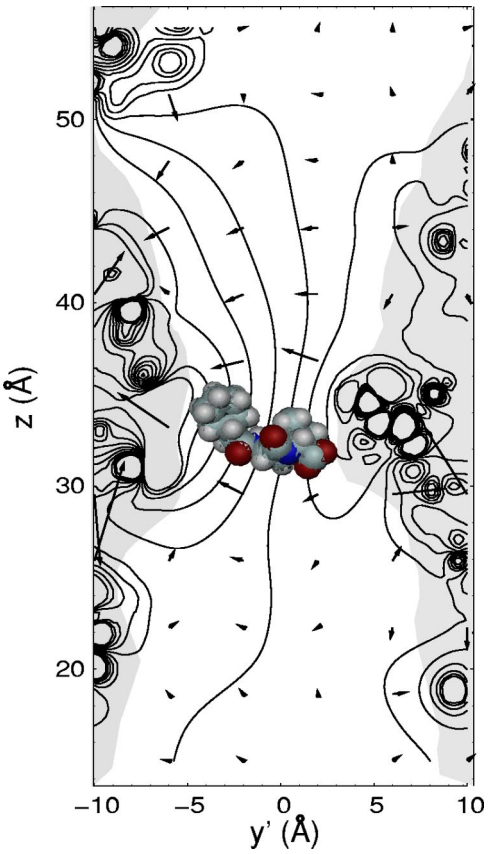

FIG. 1. Contour plot of the electric potential in the vicinity of the channel constriction (longitudinal cross section of one monomer pore), together with a vector representation of the electric field, for electrolyte concentration $C_{\mathrm{KCl}}=1$ M and no applied voltage. Thin solid lines represent sections of equipotential planes. The arrow size is proportional to the field magnitude and the shaded region corresponds to the protein. The plane shown forms 50° with the *x* axis used in the protein crystal structure [15]. Numerical calculations based on this structure used the UHBD code [31]. Computations reveal a strong transversal electric field about 0.2 V/nm at the narrowest part of the channel, in contrast with ~0.01 V/nm outside this zone. An Ampicillin molecule is also shown. See main text for details.

III. THEORY

A. Microscopic model of the system

To describe the AP behavior inside the OmpF channel constriction we use a cartesian coordinate system $\mathbf{R}\{X,Y,Z\}$ with its origin at the channel binding site where the antibiotic molecule may adsorb. As long as it is in the bound state, the AP molecule partially blocks the channel, with a significant reduction in the ionic current. The blocking is interpreted as an "event." The bound AP is treated here as a Brownian particle. The structure of OmpF is assumed to remain unchanged upon external effects such as applied voltage. Voltage V is the electric potential on *cis* side and the bulk of *trans* solution is taken as virtual ground. AP is modeled as an elongated solid of finite size. $\mathbf{r}\{x,y,z\}$ denotes the position of its mass center, and its orientation is the same as the AP dipole orientation $\{\alpha,\theta\}$ in our model (where α and θ are the angles between $\mathbf{d}_{\mathrm{AP}}$ and the positive direction of the Y axis and Z axis, respectively). During the time AP is trapped at the BS, it undergoes random thermal motion in the $\mathbf{r}$ and $\{\alpha,\theta\}$ spaces, so both mentioned vectors are time dependent. Thus the five-dimensional (5D) vectors $\mathbf{q}=\mathbf{q}\{\mathbf{r},\theta,\alpha\}$ and $\dot{\mathbf{q}}$ determine the AP phase state and the state of the total sys-

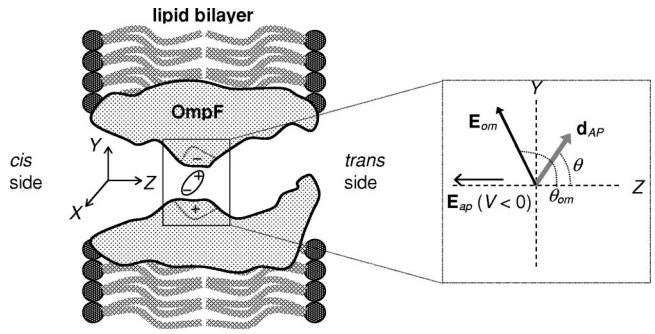

FIG. 2. Sketch of the system considered. Channel blockage takes place while Ampicillin is in the channel constriction. $\mathbf{d}_{\mathrm{AP}}$ is the AP electric dipole moment, and $\mathbf{E}_{om}$ is the electric field created by OmpF ionizable groups in constriction zone. The bulk of *trans* solution is taken as virtual ground when an external electrical field is applied. θ_{om} represents the fixed orientation of the effective OmpF electric field in the constriction zone; AP orientation, represented by its dipole moment, oscillates and θ is the instant angle with respect to the channel axis.

tem, schematically represented in Fig. 2. The applied voltage and OmpF electric charges influence this motion. The existence of a BS formally means that there is a certain domain $\boldsymbol{\omega}$ (with boundary surface $\mathbf{S}$) in the $\mathbf{q}$ space such that AP is in the bound state if $\mathbf{q} \in \boldsymbol{\omega}$. AP departs from its binding site when any point of boundary $\mathbf{S}$ is reached; i.e., $\mathbf{S}$ is treated as a perfectly adsorbing boundary. We are interested here in the influence of the applied voltage V on the mean duration of AP binding, τ_r, for a large number of events. There are a few reasons for treating this problem as a one-dimension problem. The sizes of AP and the OmpF constriction zone are similar. Therefore, owing to steric limitations, motions along x, y, and by α, are strongly limited within the channel constriction (where the BS is located). Consequently, the frequency of oscillations by x, y, and α is very high. Since we are interested here in the effect of the applied electric field $\mathbf{E}_{ap}$ (which is oriented along the Z axis) and taking into account that the measurements mentioned above [11] were made at pH 6 where $q_{\mathrm{AP}} \approx 0$, we also neglect here the oscillation by z because it depends on $\mathbf{E}_{ap}$ only if AP net charge is nonzero. Additional support follows also from the estimation of the characteristic time of the macromolecule passage across the total channel [12,34]. It was estimated as $\sim 10^{-9}$ s, which means that the characteristic time of the motion along the Z axis is five orders of magnitude shorter than that of the events considered here (10^{-4} s). Therefore, the angle θ can be regarded as the key variable of the problem. Actually, it means that the energetic potential profile of AP in the bound state has two manifest saddle points. In other words, we limit ourselves to the adiabatic approximation by assuming that the frequency of oscillation of angle θ is much smaller than all other characteristic frequencies in the system. Then, the $\boldsymbol{\omega}$ domain reduces to a 1D interval $[a,b]$ in the θ space, so that AP is in bound state if

$$a < \theta(V,t) < b. \tag{1}$$

Therefore, leaving aside how AP enters the constriction zone, we consider just the stochastic random fluctuation of the molecule tilt θ with respect to Z axis and assume that AP leaves the BS when θ reaches the values a or b. More, external forces influence on θ oscillations.

B. Determination of residence time

The mean duration of AP binding can be represented as the MFPT $T(\theta)$ for a particle with initial tilt θ_0 to reach one from two perfectly adsorbing boundaries ($\theta=a$ or $\theta=b$) (the equation from Ref. [26] is written here using our notation):

$$T(\theta_0,V) = \frac{\pi_b}{D}\int_{\theta_0}^{b} G(y,V)dy - \frac{\pi_a}{D}\int_{a}^{\theta_0} G(y,V)dy, \tag{2}$$

where V is the applied voltage and D is the AP diffusion coefficient (assumed constant) in the θ space; $\pi_a(\theta_0,\ V)$ and $\pi_b(\theta_0,\ V)$ are splitting probabilities for a particle with initial tilt θ_0 to reach boundary tilts a or b, respectively:

$$\pi_a = \pi_a(\theta_0,V) = \int_{\theta_0}^{b} e^{U(y,V)}dy \Big/ \int_{a}^{b} e^{U(y,V)}dy, \tag{3a}$$

$$\pi_b = \pi_b(\theta_0,V) = \int_{a}^{\theta_0} e^{U(y,V)}dy \Big/ \int_{a}^{b} e^{U(y,V)}dy, \tag{3b}$$

$$G(y,V) = e^{U(y,V)}\int_{a}^{y} e^{-U(z,V)}dz, \tag{3c}$$

where $U(\theta,\ V)$ is the potential of the external forces acting on the particle, in kT units. AP can gain access to the binding site with any initial orientation, $\theta_0 \in [a,b]$. Equation (2) determines the MFPT for one particular event with some specific initial orientation θ_0. The residence time τ_r—as defined in Ref. [11]—is actually the average of all events that happen during observation time t. Taking into account that $t \gg \tau_r$ and that the number of events is large, one can treat the system as well as the total set of events as being in thermal equilibrium. Then, the stationary distribution of the start points θ_0 inside the $[a,b]$ interval is determined by Boltzmann's factor and finally we obtain AP residence time as (the subindex "0" is omitted here in θ_0).

$$\tau_r(V) = \int_{a}^{b} T(\theta,V)e^{-U(\theta,V)}d\theta \Big/ \int_{a}^{b} e^{-U(\theta,V)}d\theta. \tag{4}$$

C. Potential profile of the system

Let us analyze the effect of external forces on the random motion of the AP molecule in its BS. The potential of these forces U is determined by two terms: (1) the energy of interaction of AP with the OmpF channel, U_{om}, and (2) the energy of interaction of AP with the applied electric field U_{ap}. Here U_{om} is assumed to be of electrostatic origin [11,16,23]. It is determined mainly by interaction of AP charges with the fixed charges of the protein. The strong effects of pH and ion strength of solution on the behavior of the system found by Nestorovich *et al.* [11] also support this statement. Let us denote the electric field created by OmpF

charges at the binding site by $\mathbf{E}_{om}\{E_{om}, \theta_{om}\}$ (where θ_{om} is the angle between $\mathbf{E}_{om}$ and the positive direction of the Z axis). Since τ_r is analyzed in Ref. [11] for pH=6 where $q_{\mathrm{AP}} \approx 0$ we determine U_{om} as

$$U_{om}(\theta) = -d_{AP}E_{om}F\cos(\theta - \theta_{om})/kT. \tag{5}$$

The factor F takes into account the influence of the free ions from solution on the AP-OmpF interaction, which can be modeled either in the framework of classical Debye's theory or in the framework of an "ion binding approach" [23]. In the first case, $F=F(\kappa)=(1+\kappa l_{om}/2)\exp\{-\kappa l_{om}/2\}$, where l_{om} is the effective diameter of constriction zone and κ is the inverse Debye's length of solution.[1] The second approach assumes that small ions of the solution bind to ionizable groups and neutralize the channel fixed charges and consequently change E_{om}. There are reasonable arguments to describe the screening through K^+ binding to the negative charges of OmpF [23]. In this case F becomes $F=(1+C_{\mathrm{KCl}}K_{\mathrm{K}})^{-1}$ where K_{K} is the binding constant. Note that both approaches give the same results.

We assume that the *applied electric field* $\mathbf{E}_{\mathrm{ap}}$ is directed exactly along the Z axis. Owing to the big reduction of the channel cross section in the constriction zone, the electric resistance of this narrow region is expected to be much greater than that of both channel vestibules. Besides, when AP blocks this channel eyelet, its resistance will be even higher. Therefore, it is reasonable to think that the main voltage drop of applied electric field occurs within the constriction zone—i.e., the field acting on AP is $\sim V/L_{cz}$, where L_{cz} is the effective length of the constriction zone. Hence, the contribution of this interaction to the total energy is

$$U_{ap}(\theta, V) = -d_{AP}\frac{V}{L_{cz}}\frac{\cos(\theta)}{kT}. \tag{6}$$

Summarizing Eqs. (5) and (6) one obtains the AP minimum energy orientation $\theta_{eq}(V)$ which follows from the common condition $\partial(U_{om}+U_{ap})/\partial\theta=0$, as

$$\theta_{eq}(V) = \cot^{-1}\{\cot(\theta_{om}) + V/[L_{cz}E_{om}\sin(\theta_{om})]\}. \tag{7}$$

Just this value is the most probable one for the initial orientation—i.e., $\theta_0 \approx \theta_{eq}$.

D. Determination of V_p

The value of applied voltage V_p where residence time τ_r reaches its maximum value is a pronounced characteristic of the system. The equation

$$\theta_{eq}(V_p) = (a+b)/2 \tag{8}$$

is a necessary condition for $d\tau_r(V)/dV=0$. This can be tested out either by numerical calculations or by cumbersome (but relatively simple) mathematical transformations. To illustrate the latter we show how it can be proved that all terms in the equation $d\tau_r/dV=0$ are zero if condition (8) is satisfied. As an example, let us derive the denominator of Eq. (4) with respect to voltage:

$$In(V) \equiv \frac{d}{dV}\int_a^b e^{-U(\theta,V)}d\theta = \int_a^b e^{-U}\left[\frac{\partial U}{\partial V} + \frac{\partial U}{\partial\theta}\frac{\partial\theta}{\partial V}\right]d\theta. \tag{9}$$

Now, by assuming that condition (8) is satisfied, we integrate Eq. (9) along the line $V=V_p$ where the second term within brackets in Eq. (9) is equal to zero; then,

$$In(V_p) = \int_a^b \left[\mathrm{e}^{-U}\frac{\partial U}{\partial V}\right]_{V=V_p} d\theta = \int_a^b F(\theta)d\theta = \int_{a-\theta_{eq}}^{0} F(\lambda)d\lambda + \int_0^{b-\theta_{eq}} F(\lambda)d\lambda = \int_0^{b-\theta_{eq}} F(\lambda)d\lambda - \int_0^{\theta_{eq}-a} F(\lambda)d\lambda, \tag{10}$$

where a new variable $\lambda \equiv \theta - \theta_{eq}$ is introduced and the condition $F(\lambda)=-F(-\lambda)$ is used [the latter arises from $U(\theta-\theta_{eq})=U(\theta_{eq}-\theta)$ in our model]. Therefore the total integral in Eq. (10) is equal zero if $b-\theta_{eq}=\theta_{eq}-a$—i.e., if condition (8) is true. In the same manner one can obtain that the remaining terms in $d\tau_r(V)/dV=0$ are zero if condition (8) is satisfied. Taking into account Eq. (7) one obtains, finally,

$$V_p = L_{cz}E_{om}\sin\theta_{om}\{\cot[(a+b)/2] - \cot\theta_{om}\}. \tag{11}$$

IV. RESULTS AND DISCUSSION

As is seen from Eqs. (4)–(6) the residence time variation upon applied voltage $\tau_r(V)$ depends on three OmpF structural parameters $(E_{om}, \theta_{om}, L_{cz})$ and the location of the interval $[a,b]$. As we discussed above, they can be numerically computed (except $[a,b]$) from crystallographic data [15]. For $C_{\mathrm{KCl}}=1$ M calculations yield $E_{om}=0.15-0.24$ V/nm, $\theta_{om}=70°-120°$ if negative z corresponds to the periplasmic side of the channel or $\theta_{om}=60°-110°$ if positive z corresponds to the periplasmic side,[2] and $L_{cz}=0.7-1.5$ nm. The width of the interval $[a,b]$ and its location are the adjusting parameters in our theory. As it is seen from Eq. (11) the midpoint of the interval, $(a+b)/2$, determines V_p.

In Fig. 3 we compare the relative residence time $\tau_r(V)/\tau_r^{\max}$ [here $\tau_r^{\max} \equiv \tau_r(V_p)$] obtained in the framework of our approach with experimental data from [11]. The curves show the calculations according to Eqs. (4)–(6) for different locations of the interval $[a,b]$ when $(b\text{-}a)$ is fixed. Using

[1] The application of Debye's approach in such a small space as the constriction zone is presently under discussion [16,19,22] because there are only a few ions inside this zone at any time. Since the effective time of diffusion of small ions across the constriction zone is $L^2_{\mathrm{cz}}/\mathrm{D} \sim 10^{-9}$ s $\ll \tau_{\mathrm{r}} \sim 10^{-3}$ s, then actually this approach can be applied here if the mean-field value of potentials $\varphi(\mathbf{r})$ and concentrations $C(\mathbf{r})$ at each point of the constriction zone (which are used in Debye's theory) are replaced by their time-averaged values $\langle\varphi(\mathbf{r})\rangle$ and $\langle C(\mathbf{r})\rangle$. One can easily obtain that the latter are described by the common Debye's expression, which we use here.

[2] The real OmpF orientation in channel reconstitution experiments is not known. This is the reason why we mention here two possible orientations.

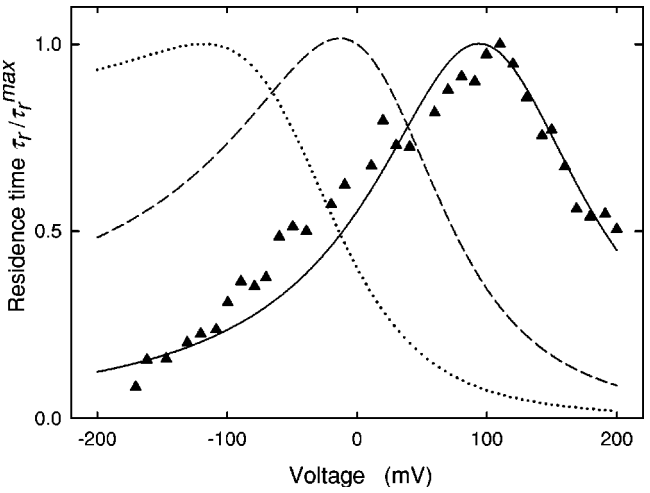

FIG. 3. Change of normalized residence time $\tau_r/\tau_r^{\max}$ with applied voltage V [here $\tau_r^{\max}=\tau_r(V_p)$]. The curves show the calculations according to Eqs. (4)–(6) for $\theta_{om}=120°$, $E_{om}=0.2$ V/nm, $L_{cz}=1.2$ nm, and $d_{\mathrm{AP}}=30$ Debye, and for different values of $(a+b)/2$: solid line corresponds to 97°, dashed line to 120°, and dotted line to 130°. Experimental data (triangles) are taken from [11].

$\tau_r(V)/\tau_r^{\max}$ enables us to bypass the problem of the diffusion coefficient D estimation. It is seen that the agreement between theory and experiment is rather good. The best fit (solid line) corresponds to $(a+b)/2=97°$ for $\theta_{om}=120°$. It should be noted that V_p is sensitive enough to the location of $(a+b)/2$—e.g., a change of 20° shifts V_p in $\sim$100 mV (dashed line). As is seen from Eq. (11) the shift of V_p to the region of positive values of applied voltage is a result of OmpF structural peculiarities—namely, a particular orientation of the OmpF electric field within its constriction—that is, $\theta_{om}\neq(a+b)/2$.

The curves shown in Fig. 3 were calculated for specific values of E_{om}, θ_{om}, and L_{cz}. The uncertainty in the estimated values of these parameters from the OmpF structure is about 20%–30%. To assess the influence of the parameter dispersion on the results we calculated V_p [Eq. (11)] using different values of E_{om}, θ_{om}, and L_{cz} for a given midpoint $(a+b)/2$. The specific values of E_{om}, θ_{om}, and L_{cz} were chosen randomly from a range of acceptable values ($E_{om}=0.1-0.2$ V/nm, $\theta_{om}=60°-120°$, $L_{cz}=0.6-1.5$ nm), assuming a uniform distribution of the probability of the specific values in their respective intervals. Here 1000 calculations were performed. V_p values obtained ranged from 0.03 to 0.2 V. However, the standard deviation from the most probable V_p value was as small as 2%. Therefore the uncertainty in the parameter estimation does not influence the final result for V_p.

Let us discuss shortly the physical meaning of the results obtained above. There are two main questions: (1) why $\tau_r(V)$ is bell shaped and (2) why V_p is located in the region of positive voltage. The physical interpretation of Eq. (4) is not trivial. It is reasonable to introduce its simplified asymptotic form that can be done in the following way. First, taking into account that θ_{eq} has the highest probability among initial orientations inside $[a,b]$ interval, one can neglect the distribution of the initial θ_0 values within interval $[a,b]$ and assume $\theta_0\approx\theta_{eq}$. Therefore $\tau_r(V)\approx T(\theta_{eq},V)$. Then, it is worth representing $T(\theta_{eq},V)$ through the rates of escape, k_a and k_b, from interval $[a,b]$ across each boundary, which can be written in their turn through the corresponding probabilities (π_a,π_b) and the heights of the energy barriers $U_b(V)=U(b,V)-U(\theta_{eq},V)$ and $U_a(V)=U(a,V)-U(\theta_{eq},V)$, as follows:

$$\frac{1}{T(\theta_{eq},V)}\approx k_a+k_b\propto\frac{\pi_a}{\exp(U_a)}+\frac{\pi_b}{\exp(U_b)}\approx\frac{(b-\theta_{eq})/(b-a)}{\exp(U_a)}+\frac{(\theta_{eq}-a)/(b-a)}{\exp(U_b)}. \quad (12)$$

Equation (12) shows the difference between the MFPT approach and the classical Eyring's rate theory which actually describes the passage across a single barrier. It transforms into Eyring's expression in the limit case of large difference between the barriers ($U_b\gg U_a$ or $U_a\gg U_b$) when the rate of escape from BS (as well as the residence time) is determined by the rate of passage across the small barrier—e.g., $\tau_r\approx[\max\{k_a,k_b\}]^{-1}\approx k_a^{-1}$ when $U_b\gg U_a$. In this case the decrease of the barrier (e.g., due to external applied voltage) always results in a decrease of the residence time. The situation is more complicated in our system because $U_b\sim U_a$. As is seen the rate of escape from interval $[a,b]$ now depends not only on the height of energy barriers but also on the initial state θ_{eq}.

Let us discuss the influence of the applied voltage V on AP escape from OmpF binding site. We start with the case of absence of voltage bias, $V=0$. The initial tilt of AP in the bound state is $\theta_0\approx\theta_{eq}=120°$ (the estimation was made by using the same parameter values as in Fig. 3). Figure 4(A) shows the potential profile $U(\theta)$ of the system (solid line in left panel) and the initial orientation of AP within the interval $[a,b]$ (arrow in right panel) in this case. The initial tilt $\theta_0=\theta_{eq}$ is closer to the boundary "*b*" than to "*a*." The probability to reach the former boundary due to thermal oscillation is higher, $\pi_b>\pi_a$. At the same time, the energy barrier U_b is lower than U_a. Therefore, the rate of escape across the *b* boundary, k_b, is higher than the rate of escape across the *a* boundary. The residence time τ_r is determined mainly by AP molecules that leave the BS through the *b* boundary. Applied voltage shifts the initial tilt θ_0 and changes the height of the energy barriers. Figure 4(B) displays the case $V>V_p>0$ when $\theta_0\approx\theta_{eq}=80°$ (for $V=0.16$ mV). Now the initial tilt of AP is closer to "*a*" and the energy barrier U_a is lower than U_b. The main contribution to τ_r comes from the AP molecules that escape from the BS through the *a* boundary. The probability to reach this boundary increases and barrier height U_a decreases as voltage becomes more positive. The rate of escape across the *a* boundary, k_a, increases significantly. As a result, $\tau_r\to0$ when $V\to\infty$. A similar behavior is found for negative voltage [Fig. 4(C)]. But in this case the initial tilt of AP moves toward the *b* boundary when V increases. This explains the bell shape of $\tau_r(V)$—i.e., why $\tau_r\to0$ when $|V|\to\infty$.

But the question is, why does τ_r grow when V increases from 0 until V_p? The peculiarity of this system is that

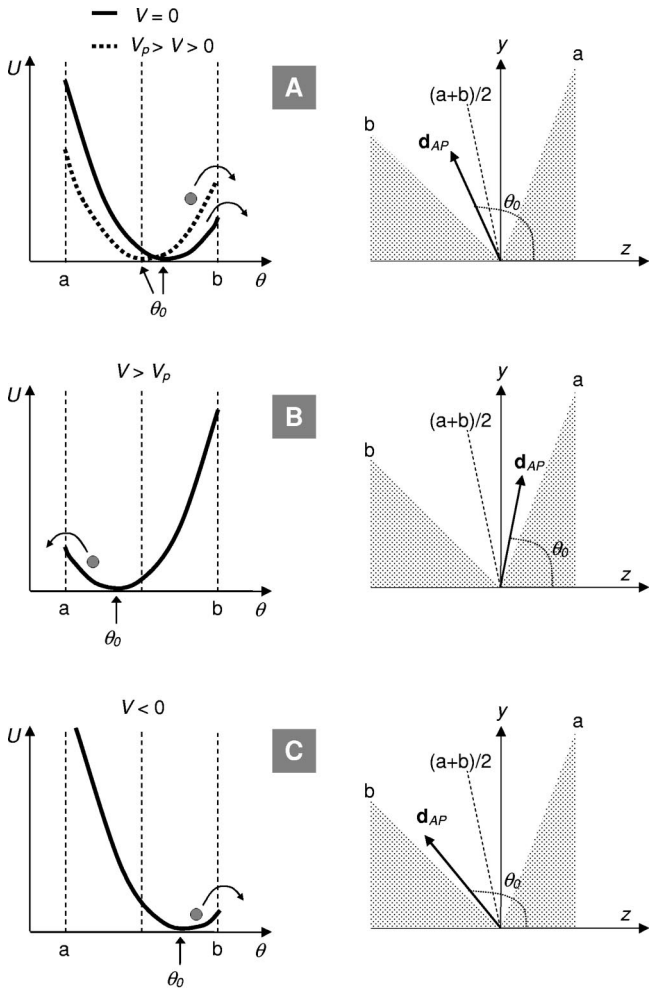

FIG. 4. Sketch of the potential profile of the system (left panel) and orientation of AP within the interval $[a,b]$ (right panel) for different values of the applied voltage: (A) $V=0$ (solid line), $V_p>V>0$ (dashed line), (B) $V>V_p>0$, (C) $V<0$. The initial tilt of AP is $\theta_0 \approx \theta_{eq}$. Here a and b are the boundaries of AP bound state, and shaded region correspond to nonbound states. See main text for details.

$\theta_{om}>(a+b)/2$ and $U_b<U_a$ for $V=0$. Any applied positive voltage increases U_b and decreases U_a always. But if the voltage is relatively small [see dashed line in Fig. 4(A)] barrier U_b is still lower than U_a and the rate of escape across the b boundary, k_b, is higher than k_a, so that the escape across the b boundary is still more favorable than the escape across the a boundary. Therefore, the main contribution to τ_r is still due to second term in Eq. (12), which decreases when V grows. But in comparison with the case of $V=0$ the rate of escape k_b is lower, therefore τ_r is greater. One can obtain that first term in Eq. (12) is a monotonically increasing function with V, but the second one is a monotonically decreasing function, therefore the cross point V_p of these functions determines the maximum of τ_r.

Summarizing, one can conclude that any positive V increases the rate of AP escape across the a boundary, k_a, but decreases the rate of AP escape, k_b, across the b boundary. One can obtain from Eq. (12) that the minimum value of the overall rate of AP escape (and the maximum of τ_r) must satisfy the condition $k_a=k_b$, which corresponds to Eq. (8). Therefore, the deviation of the $\mathbf{E}_{om}$ orientation from the value $(a+b)/2$ is the source of the asymmetry in the τ_r voltage dependence. More, according to our model, the shift of V_p to the region of positive values means that the strong transversal electric field $\mathbf{E}_{om}$ existing in the OmpF constriction has a tilt $\sim 30°$ towards the *cis* side of the channel.

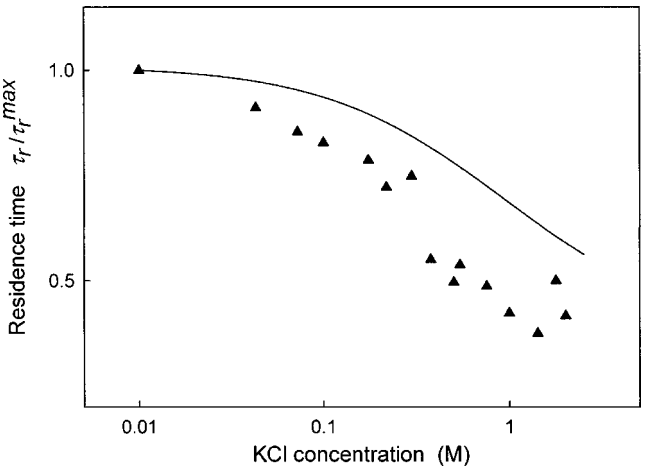

FIG. 5. Normalized residence time $\tau_r/\tau_r^{\max}$ as a function of KCl concentration for $V=-0.1$ V (here $\tau_r^{\max}=\tau_r$ for $C_{\mathrm{KCl}}=0.01$ M). The curve shows the theoretical calculations according to Eqs. (4)–(6) by using the same parameter values as in Fig. 3. Experimental data (triangles) are taken from Ref. [11].

Figure 5 shows the normalized residence time $\tau_r(V)/\tau_r^{\max}$ as a function of KCl concentration (here $\tau_r^{\max}$ corresponds to $C_{\mathrm{KCl}}=0.01$ M) for the same parameters as in Fig. 3. The same result can be obtained if we use the model of the small ion binding to ionizable groups [23] instead of Debye's theory used here. Both fitting curves overlap completely. The effect of the ionic strength of the surrounding solution on the AP binding has an obvious explanation and does not need a detailed description. Basically, the high ion concentration screens all charged residues, which interact with the AP molecule. Consequently, it decreases the interaction energies and the residence time of AP binding to OmpF. Note that theory predicts slightly bigger τ_r values than those measured experimentally. It is a result of the simplified description of the system used here. Particularly we assume that θ_{om} does not depend on solution ion strength. However, generally it may depend in the real system—e.g., due to the electric field nonuniformity in the constriction zone, which is neglected in our theory.

Our model does not distinguish the blockage of different pores of OmpF trimer but regards them completely independent. This assumption was also made in the analysis of a similar system—namely, the trimer maltoporin and sugar [12–14]. It was concluded that such assumption is acceptable in case of small or moderate concentration of solute. But in the case of high concentration the cooperative effects play probably some role.

As we mentioned in the Introduction, recently Schwarz *et al.* [14] analyzed the interaction of sugar (maltodextrin) with maltoporin channel. This system is very similar to that considered here. Its reaction on applied voltage is alike to that

for AP-OmpF. Schwarz *et al.* developed a general kinetic model which gives a phenomenological description of experimentally observable parameters. The voltage dependence of the binding constant was postulated *a priori*. Being a phenomenological model, it does not need to assume any specific physical mechanism. For example, the parameters of our model (as the parameters of any another pertinent physical theory) can be related with the parameters of their kinetic model. Nevertheless, they assumed a specific physical mechanism which can be responsible for the observed voltage dependence of binding constant of the solute to the channel—namely, the voltage-induced conformational transition of the latter. Taking into account that the system "sugar+maltoporin" is very similar to our system their hypothesis can be regarded as alternative to our approach. Generally, bound AP and OmpF constitute two-component single complex. The external effect (in our case it is the external applied voltage V) can induce (1) conformational change of AP, (2) conformational change of the channel, and (3) change of their mutual arrangement. The first point looks improbable because AP is relatively free; therefore, most probably it will move as a whole upon applied voltage. As for the second it is reasonable to expect that a similar voltage-induced conformational transition has to occur also in absence of AP and can be displayed as the variation of channel conductance and/or selectivity. This effect was not obtained in case of OmpF [35], whose voltage dependence is discussed here. Therefore it is reasonable to think that at least in this case the voltage-induced conformational change of the channel itself does not play a visible role but the third mechanism (actually suggested in the present paper) determines the obtained voltage dependences. Strictly speaking, presently it is not possible to conclude finally which mechanism is more relevant in the system considered here, because there is not enough information neither about OmpF binding site (the basis of our model) or about the voltage-dependent elasticity of charged groups of OmpF binding site (the basis of the structural hypothesis). Note that other physical models (apart from our model and that of Schwarz *et al.*) can be also assumed but our treatment seems to be the simplest one from a physical point of view.

In closing we summarize the main distinctive features of our theory among the vast literature dealing with the analysis of adsorption-desorption processes (and voltage-dependent channel gating, which can be formally described in a similar way [27]): (1) we consider the random walk of AP not in real space, but in its phase space; (2) we use the MFPT approach, which takes into account not only the dependence of energetic barriers on applied voltage but also the dependence of adsorbed particle initial state on external conditions; and (3) we represent explicitly the electric interaction of AP dipole with OmpF ionizable groups assuming that it gives the main contribution in the energy of AP-OmpF interaction. Though not essential to our development, we want to emphasize that the electric field created by the OmpF ionizable residues has been computed on the basis of the available atomic structure of this channel by using an original iterative method which estimates the apparent pKa of every single residue of the pore at any pH of bulk solution [24].

V. CONCLUSIONS

The interaction of the Ampicillin macromolecule with the OmpF channel was analyzed. We have studied the effect of the external conditions (applied voltage and ion strength of solution) on AP residence time—i.e., the mean time that the bound AP spends at the channel narrow constriction. By considering AP random thermal fluctuations within a limited region of its phase space, we determined the AP residence time as the mean first passage time to reach the boundary of the region. We assumed that the interaction of AP dipole with OmpF electric field plays the main role in these microscopic events. The angle between AP dipole moment and channel axis was selected as the main variable describing the AP state inside the channel. To compare the theoretical results with experimental data [11] we developed a model of AP-OmpF interaction assuming that electric interaction of AP dipole with OmpF electric field gives the main contribution to the energy of this interaction. This gives a simple explanation of the observation that the maximum residence time is achieved for some positive applied voltage. According to our theory the main cause of the shift is the strong transversal electric field in the channel constriction with a tilt $\sim 30°$ aside the *cis* side, which actually determines the initial orientation of AP coming into the constriction zone.

ACKNOWLEDGMENTS

V.L. thanks financial support from Secretaría de Estado de Educación y Universidades (Spain) through a grant for invited scientists (No. SAB2001-0109). V.A. thanks financial support from Fundació Caixa-Castelló (Project No. P1-1B2001-20) and from MCYT (Project No. BFM2001-3293). We thank Anatolii Beliy, Alexander Berezhkovskii, Salvador Mafé, José A. Manzanares, and Antonio Alcaraz for fruitful discussions.

[1] B. Hille, *Ionic Channels of Excitable Membranes*, 3rd ed. (Sinauer, Sunderland, MA, 2001).

[2] S. M. Bezrukov, I. Vodyanoy, and V. A. Parsegian, Nature (London) **370**, 279 (1994).

[3] R. R. Henriquez, T. Ito, L. Sun, and R. M. Crooks, Analyst (Cambridge, U.K.) **129**, 478 (2004).

[4] A. Meller, L. Nivon, E. Brandin, J. Golovchenko, and D. Branton, Proc. Natl. Acad. Sci. U.S.A. **97**, 1079 (2000).

[5] A. F. Sauer-Budge, J. A. Nyamwanda, D. K. Lubensky, and D. Branton, Phys. Rev. Lett. **90**, 238101 (2003).

[6] J. Li, M. Gershow, D. Stein, E. Brandin, and J. A. Golovchenko, Nat. Mater. **2**, 611 (2003).

[7] A. Mara, Z. Siwy, C. Trautmann, J. Wan, and F. Kamme, Nano Lett. **4**, 497 (2004).

[8] O. A. Saleh and L. L. Sohn, Nano Lett. **3**, 37 (2003).
[9] J. Li, D. Stein, C. Mcmullan, D. Branton, M. J. Aziz, and J. A. Golovchenko, Nature (London) **412**, 166 (2001).
[10] S. M. Bezrukov, J. Membr. Biol. **174**, 1 (2000).
[11] E. M. Nestorovich, C. Danelon, M. Winterhalter, and S. M. Bezrukov, Proc. Natl. Acad. Sci. U.S.A. **99**, 9789 (2002).
[12] S. M. Bezrukov, L. Kullman, and M. Winterhalter, FEBS Lett. **476**, 224 (2000).
[13] L. Kullman, M. Winterhalter, and S. M. Bezrukov, Biophys. J. **82**, 803 (2002).
[14] G. Schwarz, C. Danelon, and M. Winterhalter, Biophys. J. **84**, 2990 (2003).
[15] S. Cowan, T. Schirmer, G. Rummel, M. Steiert, R. Ghosh, R. Pauptit, J. N. Jansonius, and J. P. Rosenbusch, Nature (London) **358** 727 (1992).
[16] A. Karshikoff, V. Spassov, S. W. Cowan, R. Ladenstein, and T. Schirmer, J. Mol. Biol. **240**, 372 (1994).
[17] M. Watanabe, J. P. Rosenbusch, T. Schirmer, and M. Karplus, Biophys. J. **72**, 2094 (1997).
[18] A. Suenaga, Y. Komeiji, M. Uebayasi, T. Meguro, M. Saito, and I. Yamato, Biosci Rep. **18**, 39 (1998).
[19] T. Schirmer and P. S. Phale, J. Mol. Biol. **294**, 1159 (1999).
[20] D. P. Tieleman, G. R. Smith, P. C. Biggin, and M. S. P. Sansom, Q. Rev. Biophys. **34**, 473 (2001).
[21] K. M. Robertson and D. P. Tieleman, FEBS Lett. **528**, 53 (2002).
[22] W. Im and B. Roux, J. Mol. Biol. **322**, 851 (2002).
[23] S. Mafé, P. Ramírez, and A. Alcaraz, J. Chem. Phys. **119**, 8097 (2003).
[24] A. Alcaraz, E. M. Nestorovich, M. Aguilella-Arzo, V. M. Aguilella, and S. M. Bezrukov, Biophys. J. **87**, 943 (2004).
[25] R. Benz, A. Schmid, and G. H. Vos-Scheperkeuter, J. Membr. Biol. **100**, 21 (1987).
[26] C. W. Gardiner, *Handbook of Stochastic Methods for Physics, Chemistry, and the Natural Sciences*, corrected ed. (Springer-Verlag, Berlin, 1990).
[27] D. Sigg, H. Qian, and F. Bezanilla, Biophys. J. **76**, 782 (1999).
[28] D. K. Lubensky and D. R. Nelson, Biophys. J. **77**, 1824 (1999).
[29] J. J. Kasianowicz, E. Brandin, D. Branton, and D. W. Deamer, Proc. Natl. Acad. Sci. U.S.A. **93**, 13 770 (1996).
[30] http://www.sigmaaldrich.com (Sigma Product No. 6140, accessed on 14th January, 2004).
[31] M. E. Davis, J. D. Madura, B. A. Luty, and J. A. McCammon, Comput. Phys. Commun. **62**, 187 (1991).
[32] M. F. Sanner, A. J. Olson, and J.-C. Spehner, Biopolymers **38**, 305 (1996).
[33] DINO: Visualizing Structural Biology (2002) http://www.dino3d.org.
[34] S. M. Bezrukov, A. M. Berezhkovskii, M. A. Pustovoit, and A. Szabo, J. Chem. Phys. **113**, 8206 (2000).
[35] E. M. Nestorovich, T. K. Rostovtseva, and S. M. Bezrukov, Biophys. J. **85**, 3718 (2003).